Bioconjugate Chemistry

ARTICLE

pubs.acs.org/bc

DOTA-Amide Lanthanide Tag for Reliable Generation of Pseudocontact Shifts in Protein NMR Spectra

Bim Graham,[†] Choy Theng Loh,[§] James David Swarbrick,[†] Phuc Ung,[†] James Shin,[†] Hiromasa Yagi,[§] Xinying Jia,[§] Sandeep Chhabra,[†] Nicholas Barlow,[†] Guido Pintacuda,[‡] Thomas Huber,[§] and Gottfried Otting*[,§]

[§]Research School of Chemistry, Australian National University, Canberra ACT 0200, Australia

[†]Medicinal Chemistry and Drug Action, Monash Institute of Pharmaceutical Sciences, Parkville VIC 3052, Australia

[‡]Centre de RMN à Très Hauts Champs, ENS-Lyon, 69100 Villeurbanne, France

Supporting Information

ABSTRACT: Structural studies of proteins and protein−ligand complexes by nuclear magnetic resonance (NMR) spectroscopy can be greatly enhanced by site-specific attachment of lanthanide ions to create paramagnetic centers. In particular, pseudocontact shifts (PCS) generated by paramagnetic lanthanides contain important and unique long-range structure information. Here, we present a high-affinity lanthanide binding tag that can be attached to single cysteine residues of proteins. The new tag has many advantageous features that are not available in this combination from previously published tags: (i) it binds lanthanide ions very tightly, minimizing the generation of nonspecific effects, (ii) it produces PCSs with high reliability as its bulkiness prevents complete motional averaging of PCSs, (iii) it can be attached to single cysteine residues, alleviating the need of detailed prior knowledge of the 3D structure of the target protein, and (iv) it does not display conformational exchange phenomena that would increase the number of signals in the NMR spectrum. The performance of the tag is demonstrated with the N-terminal domain of the *E. coli* arginine repressor and the A28C mutant of human ubiquitin.

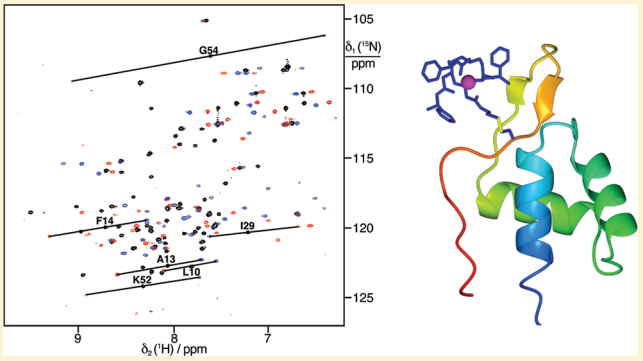

INTRODUCTION

Site-specific attachment of paramagnetic lanthanide ions to proteins produces large effects in NMR spectra that contain valuable long-range structural information.[1,2] Among the paramagnetic effects, pseudocontact shifts (PCS) stand out for their ease of measurement (as the difference in chemical shifts observed for samples labeled with, respectively, a paramagnetic or a diamagnetic lanthanide ion) and high information content (as PCSs can be observed for nuclear spins beyond 40 Å from the metal ion).

The PCS, $\Delta\delta^{PCS}$ (in ppm), of a nuclear spin can be described by[3]

$$\Delta\delta^{PCS} = \frac{1}{12\pi r^3}\left[\Delta\chi_{ax}(3\cos^2\theta - 1) + \frac{3}{2}\Delta\chi_{rh}\sin^2\theta\cos 2\varphi\right] \quad (1)$$

where $\Delta\chi_{ax}$ and $\Delta\chi_{rh}$ denote, respectively, the axial and rhombic components of the magnetic susceptibility anisotropy ($\Delta\chi$) tensor and r, and θ and φ are the polar coordinates of the nuclear spin with respect to the principal axes of the $\Delta\chi$ tensor. The limited number of parameters in eq 1 and the long-range nature of lanthanide-induced PCSs makes them powerful tools for structure determinations of protein−protein[4,5] and protein−ligand complexes (for recent reviews, see refs 6 and 7). In practice, eight parameters suffice to fit $\Delta\chi$ tensors to the 3D structure of a protein (x, y, z coordinates of the metal ion, three Euler angles to relate the orientation of the $\Delta\chi$ tensor to the frame of the protein atom coordinates, and the $\Delta\chi_{ax}$ and $\Delta\chi_{rh}$ parameters). Lanthanides are uniquely suited for PCS measurements, as different lanthanides produce different magnitudes of $\Delta\chi$ tensors while their chemical properties are very similar. This avoids chemical shift changes due to chemical differences among different paramagnetic and diamagnetic (La^{3+}, Y^{3+}, Lu^{3+}) ions.

A lanthanide ion can generate large PCSs only if it is site-specifically attached to the target protein in a rigid manner. If the tether between the lanthanide and the protein is flexible, the $\Delta\chi$ tensor associated with the lanthanide changes its orientation relative to the protein and the resulting averaging over positive and negative PCS values greatly reduces the magnitude of

Received: July 5, 2011
Revised: August 9, 2011

   dx.doi.org/10.1021/bc200353c | *Bioconjugate Chem.* XXXX, XXX, 000–000

observable PCSs. Therefore, no PCS may be observed if the tether allows substantial reorientation of the lanthanide ion with respect to the protein.

The problem of rigid lanthanide attachment can be addressed in different ways. Lanthanide chelates with two arms for attachment to two cysteine residues have been shown to minimize residual motion of the lanthanide relative to the protein.[8−10] A related strategy combines an N-terminal fusion with a lanthanide binding peptide (LBP) with a disulfide bond between the LBP and the target protein.[5,11] Engineering an LBP into the turn between two strands of a β-sheet similarly immobilizes lanthanides.[12] Another strategy coordinates the lanthanide by groups from two different sites of the protein. One group may be a small lanthanide binding tag attached to a cysteine residue, while the other group can be a carboxyl group of the protein.[13,14] Small tag molecules can also be attached to two cysteines with the aim of coordinating a single lanthanide between the two tags.[15,16] Finally, a lanthanide binding site can be engineered into the target protein by introducing amino acids with negatively charged side chains.[17] All these strategies rely on prior knowledge of the 3D structure of the target protein, at least at the site of modification.

To harness the power of PCSs for 3D structure determinations, however, it is necessary to use lanthanide tags that can be site-specifically attached without detailed knowledge of the 3D structure of the target protein. In this situation, tags with single attachment points have an advantage even if they may only incompletely immobilize the lanthanide ion. For example, LBPs with single cysteine residues have been shown to deliver large PCSs following attachment to the target protein via a disulfide bond.[18,19] The bulkiness of the tag restricts the amplitude of motion relative to the protein by steric constraints, preventing excessive averaging of the PCSs. Similarly, tags based on lanthanide complexes derived from cyclen (1,4,7,10-tetraazacyclododecane) can deliver PCSs of useful magnitudes, while providing exceptionally small dissociation constants of the lanthanide from the tag and robustness against extreme conditions of pH, temperature, and denaturants.[8,20] As a drawback, synthesis of cyclen tags can be expensive and arduous to prepare, and conformational equilibria can result in multiple sets of NMR signals.[20]

Lanthanide complexes of DOTA derivatives display two fundamental conformational equilibria.[21] The first affects the chirality of the cyclen ring. The second equilibrium affects the chirality of metal coordination by the acetate groups. Both equilibria are coupled. It has been shown that the equilibria can be pushed toward a single conformation of the lanthanide complex by incorporating chiral centers in the cyclene ring and its pendants[22] or, more simply, by turning the acetate groups of DOTA into amides with chiral amines.[23]

In the following, we present a new cyclen tag with three chiral amide groups and one nonchiral pendant for attachment to a cysteine residue of the target protein. We show that the three chiral amide pendants are sufficient to maintain a single enantiomeric conformation, as evidenced by a single set of peaks in the protein NMR spectrum, and that, even at 45 °C, the tag is free of complications arising from slow conformational exchange phenomena that have been reported for a different chiral DOTA tag.[20]

EXPERIMENTAL PROCEDURES

Tag Synthesis—(*S*)-2-Bromo-*N*-(1-phenylethyl)acetamide (1). Bromoacetyl bromide (12.7 g, 63 mmol) was added dropwise via syringe to a solution of (*S*)-1-phenylethanamine (15.3 g, 126 mmol) in DCM (200 mL) at 0 °C under nitrogen. Stirring was continued for a further 2 h at room temperature. The solution was washed with 2 N HCl (100 mL) followed by saturated brine (100 mL), then dried ($MgSO_4$), and solvent removed under reduced pressure to afford **1** (12.7 g, 83%) as a white solid. ^{1}H NMR (400 MHz, $CDCl_3$) δ 7.40−7.25 (m, 5H), 6.79 (br s, 1H), 5.12 (apparent p, J = 7.0 Hz, 1H), 3.95−3.82 (m, 2H), 1.55 (d, J = 6.9 Hz, 3H). ^{13}C NMR (101 MHz, $CDCl_3$) δ 164.7, 142.5, 128.9, 127.7, 126.2, 49.7, 29.4, 21.7. LRMS (ESI) m/z 244 (7%, $[M[^{81}Br]H]^+$), 242 (7, $[M[^{79}Br]H]^+$), 138 (10), 136 (9), 105 (100).

2,2′,2″-(1,4,7,10-Tetraazacyclododecane-1,4,7-triyl)tris-(*N*-((*S*)-1-phenylethyl)acetamide) (2). A solution of **1** (18.4 g, 76 mmol) in chloroform (500 mL) was added dropwise to a stirred mixture of cyclen (4.37 g, 25 mmol) and DIPEA (35 mL, 200 mmol) in chloroform (500 mL) under a nitrogen atmosphere at room temperature. The mixture was stirred for a further 24 h, then washed with water, and the organic phase dried over $MgSO_4$. After removal of the solvent, the residue was purified by flash chromatography (gradient from 90:10:1 to 80:20:2 EtOAc/MeOH/NH_3) to afford the product (10.2 g, 61%) as a thick, light yellow oil. ^{1}H NMR (400 MHz, DMSO) δ 8.36 (d, J = 8.0 Hz, 2H), 8.26 (d, J = 7.8 Hz, 1H), 7.33−7.26 (m, 12H), 7.25−7.16 (m, 3H), 4.98−4.85 (m, 3H), 3.15−3.00 (m, 6H), 2.73−2.43 (m, 16H), 1.41−1.30 (m, 9H). ^{13}C NMR (101 MHz, DMSO) δ 169.7(2), 169.6(8), 144.7, 144.4, 128.2, 128.2, 126.6, 126.5, 126.0, 126.0, 57.7, 55.9, 52.7, 52.3, 50.9, 47.7, 47.6, 46.4, 22.5, 22.4. LRMS (ESI) m/z 656 (85%, $[M+H]^+$), 329 (100, $[M+2H]^{2+}$).

2-Chloro-*N*-(2-(pyridin-2-yldisulfanyl)ethyl)acetamide (3). To a stirred solution of 2-(pyridin-2-yldisulfanyl)ethanamine hydrochloride (3.00 g, 13.5 mmol) and chloroacetic acid (1.28 g, 14 mmol) in 1:10 dichloromethane/acetonitrile (50 mL) was added DIPEA (7.0 mL, 400 mmol) and BOP (6.63 g, 15 mmol). The reaction mixture was stirred overnight at room temperature under nitrogen. Upon completion of the reaction, the solvent was removed under reduced pressure and the resulting crude product was dissolved in saturated $NaHCO_3$ solution (150 mL) and washed with ether (3 × 100 mL). The combined organic layers were washed with saturated brine, dried ($MgSO_4$), and the solvent removed under reduced pressure. Flash chromatography (30:70 ethyl acetate/petroleum spirit) afforded **2** (2.80 g, 79%) as a slightly yellow oil. ^{1}H NMR (400 MHz, $CDCl_3$) δ 8.56 (ddd, J = 4.9, 1.8, 0.9 Hz, 1H), 8.26 (br s, 1H), 7.60 (ddd, J = 8.0, 7.4, 1.8 Hz, 1H), 7.47 (dt, J = 8.1, 1.0 Hz, 1H), 7.14 (ddd, J = 7.4, 4.9, 1.1 Hz, 1H), 4.09 (s, 2H), 3.67−3.56 (m, 2H), 2.97−2.87 (m, 2H). ^{13}C NMR (101 MHz, $CDCl_3$) δ 166.3, 159.1, 150.2, 137.0, 121.5, 121.4, 42.9, 38.9, 37.6. LRMS (ESI) m/z 265 (40%, $[M[^{37}Cl]H]^+$), 263 (100, $[M[^{37}Cl]H]^+$).

2,2′,2″-(10-(2-Oxo-2-(2-(pyridin-2-yldisulfanyl)ethylamino)-ethyl)-1,4,7,10-tetraazacyclododecane-1,4,7-triyl)tris(*N*-((*S*)-1-phenylethyl)acetamide) (C1). A mixture containing **3** (1.40 g, 2.1 mmol), **2** (1.00 g, 3.8 mmol), and DIPEA (610 μL, 3.8 mmol) in acetonitrile (50 mL) was stirred at room temperature for 48 h. The resultant white precipitate was filtered and dried to afford C1 (0.65 g, 35%) as a white solid. Evaporation of the filtrate and purification of the residue by flash chromatography (90:10:1 DCM/MeOH/NH_3) afforded a further crop of the product (0.78 g, 41%). ^{1}H NMR (400 MHz, DMSO) δ 8.46−8.42 (m, 1H), 8.28 (t, J = 5.8 Hz, 1H), 8.19 (d, J = 8.1 Hz, 1H), 8.15 (d, J = 8.1 Hz, 2H), 7.83−7.76 (m, 1H), 7.73 (dt, J = 8.1, 1.0 Hz, 1H), 7.33−7.25 (m, 12H), 7.24−7.16 (m, 4H), 5.00−4.86 (m, 3H),

dx.doi.org/10.1021/bc200353c |*Bioconjugate Chem.* XXXX, XXX, 000–000

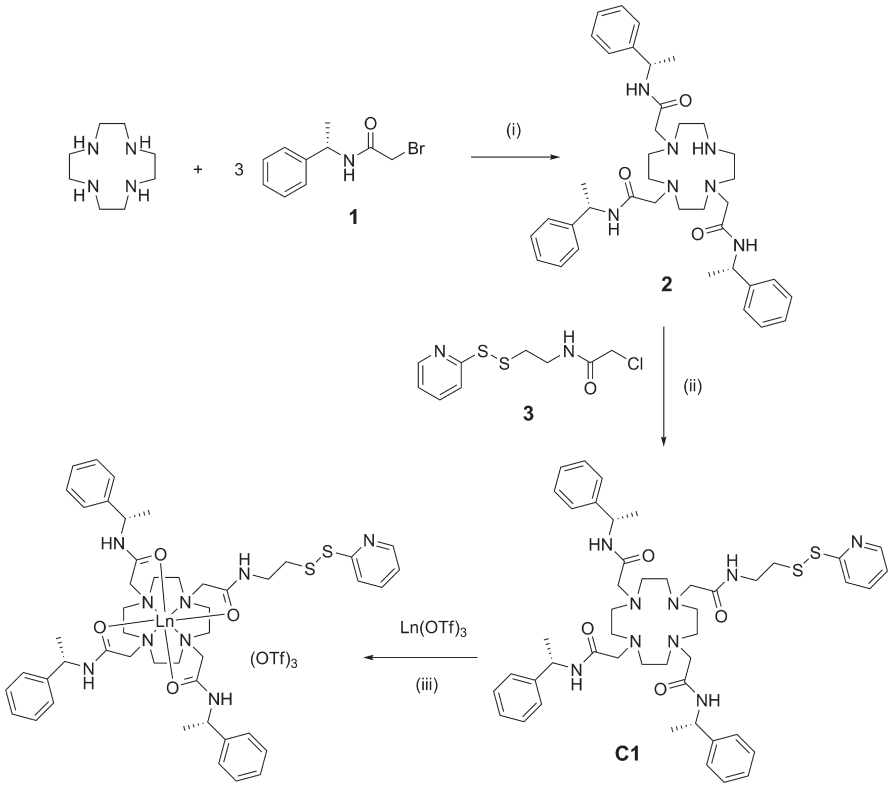

Figure 1. Synthesis of C1 tag and lanthanide complexes. Conditions: (i) DIPEA, chloroform, RT, O/N; (ii) DIPEA, acetonitrile, RT, 2 d; (iii) acetonitrile, reflux, O/N.

3.41−3.32 (m, 2H), 3.07−2.96 (m, 6H), 2.93−2.83 (m, 4H), 2.75−2.42 (m, 16H), 1.43−1.28 (m, J = 8.8, 7.1 Hz, 9H). ^{13}C NMR (101 MHz, DMSO) δ 170.6, 169.4, 169.4, 159.1, 149.6, 144.4, 144.3, 137.7, 128.2, 126.6, 126.0, 126.0, 121.2, 119.3, 58.1, 57.9, 57.6, 53.6, 53.3, 52.9, 47.6, 37.6, 37.4, 22.2, 22.1. HRMS (ESI): m/z: calcd for$[M+H]^+$ $C_{47}H_{64}N_9O_4S_2$: 882.4517, found: 882.4555.

Formation of Metal Complexes. As binding of lanthanides to DOTA-type cyclen derivatives is extremely slow and requires heating, we did not attempt to exchange the metal ion from tagged protein samples. To produce protein samples with different lanthanides, the C1 tag was prepared with different paramagnetic and diamagnetic ions (Tb^{3+}, Tm^{3+}, Yb^{3+}, Y^{3+}) by heating the tag in acetonitrile with a molar equivalent of the respective metal triflate salts overnight at 80 °C, followed by freeze−drying to afford off-white powders. Stock solutions of the C1−lanthanide complexes were prepared in water with concentrations of up to 20 mM.

Tagging Reaction. Uniformly ^{15}N/^{13}C-labeled samples of the N-terminal domain of the *E. coli* arginine repressor (ArgN) were produced on M9 minimum medium as described.[24] A 0.2 mM solution of ArgN in NMR buffer (20 mM MES, pH 6.6) was reduced by 5 equiv of DTT and subsequently washed with NMR buffer using a Millipore ultrafilter with a molecular weight cutoff of 3 kDa. The solution was added to a 3-fold excess of tag in NMR buffer to yield a total volume of 0.5 mL and the mixture was incubated at room temperature for 5 h. The reaction mixture was washed again with NMR buffer and concentrated to a final volume of 0.5 mL.

Uniformly ^{15}N-labeled samples of the mutant A28C of human ubiquitin were prepared as described.[15] DTT reduction of the thiol was as above for ArgN followed by passage over a PD10 column equilibrated with degassed NMR buffer (50 mM HEPES pH 7.5). A 15-fold excess of tag was added from a 20 mM stock solution in water to an approximately 50 μM solution of the protein and left for 3 h at room temperature and then overnight at 3 °C. Excess tag was removed by passage over a PD10 column and the sample concentrated using a Millipore ultrafilter to a final protein concentration of about 70 μM.

NMR Spectra. NMR spectra were recorded at 25 °C on 600 MHz NMR spectrometers equipped with cryogenic probes (Bruker Avance and Varian INOVA in the case of ArgN and ubiquitin(A28C), respectively). ^{15}N-HSQC, 3D HNCA, and HN(CO)CA spectra were recorded from differently tagged ArgN. ^{15}N-fast-HSQC spectra were recorded from differently tagged ubiquitin(A28C), and a 3D NOESY−^{15}N-HSQC spectrum was recorded from the ubiquitin(A28C)−C1-Y^{3+} complex. Resonance assignments of paramagnetic NMR spectra were supported by the program *Numbat*[25] to fit $\Delta\chi$ tensors to a set of unambiguously assigned PCSs and predict the PCSs of unassigned paramagnetic cross-peaks in several rounds of $\Delta\chi$ tensor fitting and resonance assignments.

Fitting of $\Delta\chi$ Tensors. $\Delta\chi$ tensors were fitted to the first conformer of the NMR structure of ArgN (PDB accession code 1AOY[24]) following a previously described protocol.[26,27] Briefly, the structure of ArgN with the C1 tag was modeled using the enantiomeric mirror image of the crystal coordinates of the DOTA-tetraamide Gd^{3+} complex with 1-phenylethyl amine (DOTAMPh, CSD accession code EQOZUF[28]). One of the 1-phenylethyl groups of the DOTAMPh molecule was changed to a 2-thioethyl group, which was connected via a disulfide bond to the sulfur of Cys68 of ArgN. 4×10^6 different conformations

dx.doi.org/10.1021/bc200353c |*Bioconjugate Chem.* XXXX, XXX, 000–000

were generated by randomly changing the χ_1 and χ_2 angles of Cys68 and the dihedral angles of the disulfide bond and ethylene tether, using dihedral angles of 60°, −60°, and 180° for the C−C bonds and dihedral angles of −90° or 90° for the S−S bond, with an uncertainty range of ±10°. Conformations producing steric clashes with the protein were excluded. The remaining 2287 conformers were used to fit $\Delta\chi$ tensors to the experimental PCSs. The final $\Delta\chi$ tensor was taken to be the one obtained with the conformation producing the best least-squares fit to the experimentally observed PCS data. As a measure of the precision of the $\Delta\chi$-tensors and metal positions, the fits to each of the 2287 model conformers were repeated 100 times, omitting 20% of the data from each metal ion in a Monte Carlo protocol.[25]

Fitting of $\Delta\chi$ tensors to the ubiquitin mutant A28C followed the same protocol as for ArgN. The fits used the first conformer of the NMR structure (PDB accession code 1D3Z[29]). 2897 conformers were obtained that were free of steric clashes between tag and protein.

RESULTS

Synthesis of the C1 Tag and Its Lanthanide Complexes. Figure 1 shows the synthetic route used to prepare the "conjugation ready" C1 tag from 1,4,7,10-tetraazacyclododecane (cyclen). This involved the sequential attachment of the three chiral amide groups and one nonchiral pendant via reaction with α-haloacetamide derivatives of (*S*)-1-phenylethanamine and 2-(pyridin-2-yldisulfanyl)ethanamine, respectively. Although chromatography was required at both stages to remove impurities, the synthesis avoided the need for protection groups and afforded the tag in good overall yield. The lanthanide complexes of C1 were readily prepared by refluxing 1:1 mixtures of the ligand and metal triflate salts, $Ln(OTf)_3$ (Ln = Dy^{3+}, Tb^{3+}, Tm^{3+}, Yb^{3+}, Y^{3+}), in acetonitrile overnight.

Tagging Reaction and Protein NMR Assignments. The C1 tag was attached to ArgN by adding the protein to a 3-fold excess of tag rather than adding tag to protein, to avoid the possibility of disulfide-bond formation between different protein molecules which could arise from disulfide exchange. The reaction reproducibly delivered tagged ArgN with greater than 95% yield. Samples were produced with tags loaded with different lanthanides (Dy^{3+}, Tb^{3+}, Tm^{3+}, Yb^{3+}) or a diamagnetic metal (Y^{3+}).

The C1 tag was attached to the ubiquitin mutant A28C using a similar protocol or a large excess of tag as described in the Experimental Procedures. Reaction yields increased with the duration of incubation (from hours to days) with the C1 tag. An overnight reaction at 3 °C (i.e., conditions suitable for less stable proteins) yielded 80−90% of tagged ubiquitin. Even the use of a large excess of tag produced no evidence for disulfide mediated protein dimerization.

The backbone NMR resonances of paramagnetic and diamagnetic ArgN-C1 complexes were assigned using 3D HNCA and HN(CO)CA spectra. The resonance assignments obtained are compiled in Supporting Information Table S1. Chemical shift changes in ArgN and ubiquitin(A28C) tagged with diamagnetic Y^{3+} tags were limited to amides in the vicinity of the cysteine residue, indicating that the tags did not significantly alter the protein structures. The resonance assignments of the diamagnetic ubiquitin(A28C)−C1−Y^{3+} complex were established by a 3D NOESY−^{15}N-HSQC spectrum. For either protein, resonance assignments of the paramagnetic samples were aided by the fact that the PCSs produced by different lanthanides

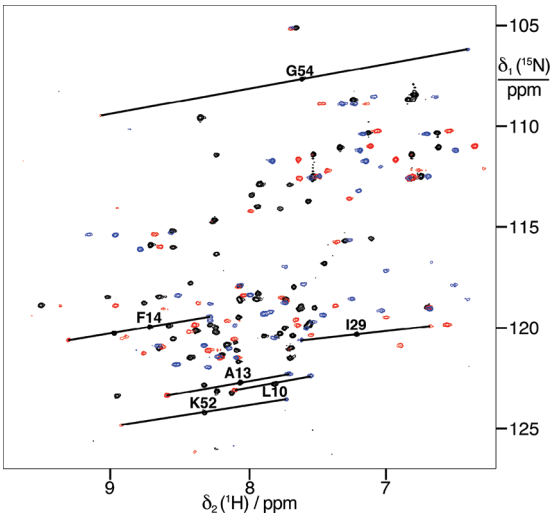

Figure 2. Superimposition of ^{15}N-HSQC spectra of 0.2 mM solutions of uniformly ^{13}C/^{15}N-labeled N-terminal domain of the *E. coli* arginine repressor ligated at Cys68 with the C1 tag loaded with Y^{3+} (black peaks), Tb^{3+} (red), or Tm^{3+} (blue). All spectra were recorded at 25 °C on a 600 MHz NMR spectrometer in a 20 mM MES buffer, pH 6.6. Selected diamagnetic cross-peaks are labeled with their resonance assignments and connected by lines with their paramagnetic partners.

displaced the cross-peaks along almost straight lines. Supporting Information Table S2 shows the experimentally determined PCSs of ubiquitin(A28C).

PCS Measurements and $\Delta\chi$ Tensors. Pronounced PCSs were observed in the complexes of ArgN and ubiquitin(A28C) tagged with C1 containing Dy^{3+}, Tb^{3+}, Tm^{3+}, or Yb^{3+}. All samples produced high-quality NMR spectra (Figure 2 and Supporting Information Figure S2). There was no evidence for conformational heterogeneity of the tag or slow conformational exchange, neither in the C1−Yb^{3+} tag alone (Figure S1) nor in the ubiquitin(A28C) mutant tagged with C1−Yb^{3+} and measured with high signal-to-noise ratio (Figure S3). No minor conformational species appeared at 45 °C (Figures S1 and S3).

$\Delta\chi$ tensors were fitted to the experimental PCSs using the first conformer of the NMR structure of ArgN[24] with the covalent structure of the tags crafted onto it via a disulfide bond linkage to Cys68. Table 1 shows the parameters of the fitted $\Delta\chi$ tensors. The tensors were sufficiently large to generate PCSs of up to 0.13 ppm at the site most remote from Cys68 (the amide proton of Asp39 in the C1(Tb)-tagged protein which is 32 Å from the site of the metal ion).

Fits of the $\Delta\chi$ tensors to the NMR structure of ubiquitin[29] produced smaller tensors than in the case of ArgN (Supporting Information Table S3), suggesting that the exposure of Cys28 on the surface of the protein permits a greater amplitude of motion for the tag (Figure S4; the calculated solvent accessibility of Cys68 of ArgN is about 7% and is 22% for Cys28 of ubiquitin(A28C)). As in the case of ArgN, however, the C1 tag produced significantly larger $\Delta\chi$ tensors than a previously used NTA derivative (N^{α},N^{α}-bis(carboxymethyl)-L-cysteine) that is a much smaller molecule with a shorter linker.[15]

Back-calculated and experimental PCSs correlated closely for ArgN and ubiquitin (Figure 3). Remarkably, the correlation was better for ubiquitin than for ArgN despite the greater conformational freedom of the C1 tag on the surface of ubiquitin, indicating that tag mobility is a lesser impediment to good fits of PCS data than structure quality.

dx.doi.org/10.1021/bc200353c |*Bioconjugate Chem.* XXXX, XXX, 000–000

Table 1. $\Delta\chi$ Tensors of Different Metal Ions Bound to ArgN-C1[a]

metal ion	$\Delta\chi_{ax}$ /10^{-32} m^3	$\Delta\chi_{rh}$ /10^{-32} m^3	Q^b	tensor axis	coordinates of tensor axes		
Dy^{3+}	−29	−11	0.08	*x*	−0.302	−0.248	0.921
	(−42/−25)	(−13/−7)		*y*	0.941	0.077	0.329
				z	−0.152	0.966	0.210
Tb^{3+}	−27	−4	0.14	*x*	−0.235	−0.064	−0.965
	(−37/−21)	(−9/−1)		*y*	−0.935	−0.240	0.261
				z	−0.249	0.969	0.001
Tm^{3+}	37	12	0.21	*x*	−0.833	−0.450	0.322
	(26/59)	(3/24)		*y*	0.439	−0.183	0.880
				z	−0.337	0.874	0.350
Yb^{3+}	13	3	0.18	*x*	−0.808	−0.444	0.388
	(10/19)	(0/7)		*y*	0.495	−0.154	0.855
				z	−0.320	0.883	0.344

[a] The tensors are listed in their unique tensor representation (UTR)[25] as obtained by fitting of the PCSs of Table S1 to ArgN (PDB ID 1AOY model 1)[24] simultaneously using the PCSs induced by Dy^{3+}, Tb^{3+}, Tm^{3+}, and Yb^{3+} and a common metal position. The fits used PCSs of amide protons in structurally well-defined regions of the protein (residues 8−20, 26−37, 43−52). The covalent structure of the tag was taken into account as described in the main text. The orientations of the tensor axes are given as unit vectors with respect to the origin (0, 0, 0). Uncertainty ranges (shown in brackets) were obtained by a Monte Carlo error analysis that randomly omitted 20% of the PCSs (100 trials for each of 2287 modeled tag conformations). The coordinates of the common metal position in the best fit using 100% of the PCSs were (13.705, 11.580, 0.445). A small fraction (9%) of the best solutions in the Monte Carlo trials positioned the metal in a group about 4 Å from this position. These solutions were omitted from the error analysis. In the remaining solutions, the metal was displaced by <1.9 Å. [b] *Q*-factor calculated as root-mean-square deviation between measured and predicted PCSs divided by the root-mean-square of the measured PCSs. The *Q*-factor of the simultaneous four-metal fit is 0.16.

DISCUSSION

Our results indicate that the C1 tag reliably produces PCSs following attachment to single cysteine residues. This is an important advantage over DPA tags[13,14,27] or IDA and NTA tags[15,16] that often generate vanishingly small PCSs if the metal ion is not coordinated by an additional carboxyl group from the protein, as mobility of the tether to the protein invariably reduces the magnitude of the PCSs observed in the protein. The reliability with which the C1 tag generates PCSs can be attributed to its bulkiness, which limits the amplitude of reorientational motions of the DOTA moiety relative to the protein. For comparison, no PCSs could be generated with lanthanides in the ubiquitin (A28C) mutant tagged with the much smaller 4MDPA tag[27] (data not shown), despite there being only a single rotatable bond in the linker between the lanthanide and the disulfide bond. Reliable generation of PCSs in the absence of structural information is an essential prerequisite before the power of PCS data can be harnessed for 3D structure determinations of proteins.

Generation of sizable PCSs in the target protein is greatly aided by an intrinsically large $\Delta\chi$ tensor of the lanthanide tag. Remarkably large paramagnetic shifts have been reported for the Yb^{3+} complex of the symmetrical parent compound of the C1 tag, DOTAMPh, which has 1-phenylethylacetamide pendants attached to all four nitrogens of the cyclen ring.[23] As the cyclen protons are separated from the lanthanide by only a few bonds, it is unclear, however, which fraction of the paramagnetic shifts in DOTAMPh must be attributed to contact shifts rather than PCSs. In a protein tagged with C1, however, contact shifts can be neglected for protons that are sufficiently far from the metal to yield observable NMR signals. Remarkably, the $\Delta\chi_{ax}$ value of 13 × 10^{-32} m^3 determined for the ArgN-C1(Yb^{3+}) complex (Table 1) is almost two times greater than any that has been reported for Yb^{3+} complexes of calbindin D_{9k},[30] CLaNP-5.2,[8,9] lanthanide binding peptides,[19] or DPA tags.[13,19,27] Correspondingly large residual dipolar couplings (RDC) could be observed on an 800 MHz NMR spectrometer, with $^1D_{HN}$ RDCs of up to 20.3 Hz measured for ArgN-C1(Tm^{3+}) at 25 °C. Maximal $^1D_{HN}$ RDC values greater than 20 Hz are hallmarks of the best lanthanide tags currently available.[8,20,31,32] Under the conditions of our RDC measurements, a maximal $^1D_{HN}$ value of about 20 Hz would be predicted for the $\Delta\chi_{ax}$ value of 37 × 10^{-32} m^3 associated with ArgN-C1(Tm^{3+}) (Table 1). This close agreement between predicted and experimental maximal RDC values would suggest that the tag has little conformational freedom. Large uncertainty ranges, however, were associated with the $\Delta\chi$ tensor determinations, which may be attributed to the fairly long distance of the metal from the protein surface (8 Å from the sulfur of the cysteine residue; Figure 4) and similar directions of the principal tensor axes of the different metals (Table 1).

In contrast to the situation encountered with RDCs, where the average of different alignment tensors can be represented by a single average tensor, an ensemble of different $\Delta\chi$ tensors from different metal positions cannot be approximated well by a single average tensor, at least not close to the metal ion, since PCSs are distance-dependent. At greater distances from the paramagnetic center, however, the approximation by an average $\Delta\chi$ tensor is much better, as different tag conformations have a smaller relative influence on the distance between nuclear spins and paramagnetic center. Therefore, even if mobility of the tag leads to a reduced average $\Delta\chi$ tensor, this tensor still yields useful structural restraints at greater distances from the metal ion, as long as it fits the experimentally observed PCSs in those regions of the protein. The large intrinsic $\Delta\chi$ tensor associated with the C1 tag thus makes it a useful tool for protein structure analysis even in the presence of substantial averaging as observed for the ubiquitin A28C mutant. Notably, PCSs could be measured for almost all peaks of ubiquitin (Supporting Information Figure S2) and even using all PCSs from residues 2−72 produced a better fit of back-calculated versus experimental PCSs for ubiquitin than for ArgN for which only a NMR structure determined by NOEs and *J* couplings is available (Figure 3).

dx.doi.org/10.1021/bc200353c |*Bioconjugate Chem.* XXXX, XXX, 000–000

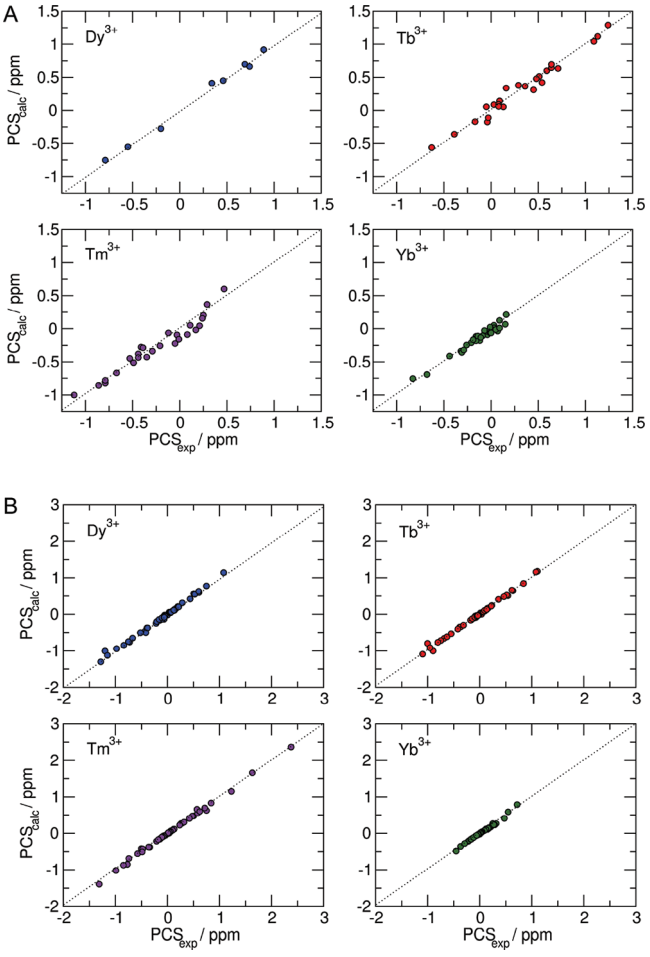

Figure 3. Correlations between back-calculated and experimental pseudocontact shifts of (A) the N-terminal domain of the *E. coli* arginine repressor and (B) ubiquitin obtained by the fits of Table 1 and Supporting Information Table S3, respectively.

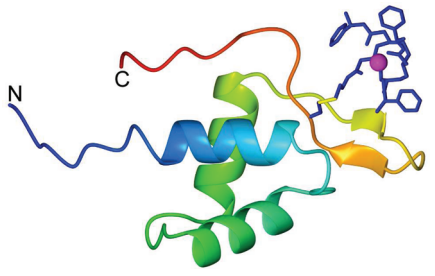

Figure 4. Model of the N-terminal domain of the *E. coli* arginine repressor with a C1-lanthanide complex bound to Cys68. The model represents the best fit of the PCSs to the first conformer of the NMR structures (PDB ID 1AOY[24]). The structure of the tag was derived from the crystal coordinates of a DOTA-tetraamide Gd^{3+} complex as described in the main text. The lanthanide ion is represented by a magenta sphere. The disulfide bond of the linker is highlighted in yellow. The N- and C-termini are labeled. The side chain of Cys68 and the tag are shown in a heavy atom representation.

$\Delta\chi$ tensor fits easily generate large uncertainty ranges for metal tags on protein surfaces, as the metal position must be determined along with five other tensor parameters (Euler angles and axial and rhombic components). For example, an unrealistically large distance of the metal from the protein can often be quite readily compensated for by a correspondingly larger tensor. To avoid such artifacts, we used a fitting procedure that explicitly restricts metal coordinates to positions that are compatible with the covalent structure of the tag and its steric requirements. Unless the tag is completely immobilized, however, the particular tag conformation producing the best fit must not be taken too literally, as the fitting does not consider the different rotamers of the linker moiety that may lead to the average metal position found.

The C1 tag carries the same ethylene thio linker as the previously published cyclen tags DOTA-M8[20] and CLaNP-5.1.[8] In the case of the DOTA-M8 tag, 15−20% of the tag was observed to assume a second conformation at 25 °C, which was tentatively attributed to cis−trans isomerization of the amide bond of the tether. This percentage rose to 50% at 50 °C.[20] In contrast, no second conformational species was reported for the CLaNP-5.1 tag[8] and we found no evidence for slow conformational exchange in the C1 tag either, not even at 45 °C (Supporting Information Figures S1 and S3). The C1 tag is thus suitable for measurements at elevated temperatures.

For the CLaNP-5.1 tag, data have been reported only for a single metal ion (Yb^{3+}) and protein site,[8] making comparisons difficult. We would expect the C1 tag to be less prone to PCS averaging because of its greater bulkiness. Compared to the even bulkier lanthanide binding peptides,[18,19] the C1 tag, like most DOTA-type tags, binds lanthanide ions much more tightly, is more resistant to unfolding under nonphysiological conditions, and is easier to use, as it is synthesized with an activated disulfide bond. The high lanthanide affinity of DOTA-type tags (dissociation constants of 100 pM have been reported for lanthanide complexes of cyclen with *N*-acetamide pendants, DOTAM[33]) is a decisive advantage for experiments with metalloproteins, where a kinetically less inert metal binding tag could lead to equilibration between the metals of the protein and the tag, for studies of compounds that display high natural affinities for lanthanides, such as DNA and RNA, and for EPR experiments with Gd^{3+} that depend on the absence of unbound Gd^{3+} ions.[34]

The parent compound of the C1 tag, DOTAMPh, forms a square antiprismatic complex[23] that completely encases the lanthanide ions except for a single coordination site for a water molecule.[35] The poor accessibility of the lanthanide is an advantage in interaction studies, where more solvent-exposed metal ions could produce misleading results by direct interactions between the metal and the interaction partner. The C1 tag thus carries great promise for lead compound development by fragment-based drug design, where PCSs observed for weakly binding fragments can be used to define their binding site, orientation, and structure.[36,37]

Using different lanthanides in the same protein-tag construct generates $\Delta\chi$ tensors of different magnitude, but the orientations of the principal axes of the tensors usually vary little.[13,30,38] It is a distinct possibility that a tag produced with opposite chirality (using (*R*)-1-phenylethanamine instead of (*S*)-1-phenylethanamine) may generate different tensor orientations relative to the protein. PCS data measured with both enantiomeric tags could thus deliver two independent sets of restraints to position nuclear spins relative to the protein.

In conclusion, the new lanthanide tag presented here displays an attractive combination of properties, including reliable generation of PCSs, conformational homogeneity, and tight lanthanide binding. We anticipate that it will become an important tool

dx.doi.org/10.1021/bc200353c |*Bioconjugate Chem.* XXXX, XXX, 000–000

for assessing the structure of biological macromolecules by NMR spectroscopy.

■ ASSOCIATED CONTENT

Supporting Information. ^{1}H NMR spectrum of the C1−Yb^{3+} complex, chemical shifts of ArgN tagged with C1 loaded with different metal ions, ^{15}N-HSQC spectra of ubiquitin (A28C) tagged with C1 loaded with different metal ions, PCSs of ubiquitin (A28C) tagged with C1 metal complexes, $\Delta\chi$ tensors of ubiquitin (A28C) tagged with C1 metal complexes, model of the C1 tag bound to Cys28 in ubiquitin (A28C). This material is available free of charge via the Internet at http://pubs.acs.org.

■ AUTHOR INFORMATION

Corresponding Author

*Gottfried Otting, Research School of Chemistry, Australian National University, Canberra, ACT 0200 (Australia). Fax: +61-2-61250750. E-mail: gottfried.otting@anu.edu.au.

■ ACKNOWLEDGMENT

Financial support by the Australian Research Council, including a Future Fellowship to T. H., is gratefully acknowledged.

■ REFERENCES

(1) Pintacuda, G., John, M., Su, X.-C., and Otting, G. (2007) NMR structure determination of protein-ligand complexes by lanthanide labelling. *Acc. Chem. Res. 40*, 206–212.

(2) Otting, G. (2008) Prospects for lanthanides in structural biology by NMR. *J. Biomol. NMR 42*, 1–9.

(3) Bertini, I., Luchinat, C., and Parigi, G. (2002) Magnetic susceptibility in paramagnetic NMR. *Prog. Nucl. Magn. Reson. Spectrosc. 40*, 249–273.

(4) Keizers, P. H. J., Mersinli, B., Reinle, W., Donauer, J., Hiruma, Y., Hannemann, F., Overhand, M., Bernhardt, R., and Ubbink, M. (2010) A solution model of the complex formed by adrenodoxin and adrenodoxin reductase determined by paramagnetic NMR spectroscopy. *Biochemistry 49*, 6846–6855.

(5) Saio, T., Yokochi, M., Kumeta, H., and Inagaki, F. (2010) PCS-based structure determination of protein-protein complexes. *J. Biomol. NMR 46*, 271–280.

(6) Keizers, P. H. J., and Ubbink, M. (2011) Paramagnetic tagging for protein structure and dynamics analysis. *Prog. Nucl. Magn. Reson. Spectrosc. 58*, 88–96.

(7) Otting, G. (2010) Protein NMR using paramagnetic ions. *Annu. Rev. Biophys. 39*, 387–405.

(8) Keizers, P. H. J., Desreux, J. F., Overhand, M., and Ubbink, M. (2007) Increased paramagnetic effect of a lanthanide protein probe by two-point attachment. *J. Am. Chem. Soc. 129*, 9292–9293.

(9) Keizers, P. H. J., Saragliadis, A., Hiruma, Y., Overhand, M., and Ubbink, M. (2008) Design, synthesis, and evaluation of a lanthanide chelating protein probe: CLaNP-5 yields predictable paramagnetic effects independent of environment. *J. Am. Chem. Soc. 130*, 14802–14812.

(10) Vlasie, M. D., Comuzzi, C., van den Nieuwendijk, A. M., Prudêncio, M., Overhand, M., and Ubbink, M. (2007) Long-range-distance NMR effects in a protein labeled with a lanthanide-DOTA chelate. *Chem.—Eur. J. 13*, 1715–1723.

(11) Saio, T., Yokochi, M., and Inagaki, F. (2009) Two-point anchoring of a lanthanide-binding peptide to a target protein enhances the paramagnetic anisotropic effect. *J. Biomol. NMR 44*, 157–166.

(12) Barthelmes, K., Reynolds, A. M., Peisach, E., Jonker, H. R. A., DeNunzio, N. J., Allen, K. N., Imperiali, B., and Schwalbe, H. (2011) Engineering encodable lanthanide-binding tags into loop regions of proteins. *J. Am. Chem. Soc. 133*, 808–819.

(13) Man, B., Su, X.-C., Liang, H., Simonsen, S., Huber, T., Messerle, B. A., and Otting, G. (2010) 3-Mercapto-2,6-pyridinedicarboxylic acid, a small lanthanide-binding tag for protein studies by NMR spectroscopy. *Chem.—Eur. J. 16*, 3827–3832.

(14) Su, X.-C., Man, B., Beeren, S., Liang, H., Simonsen, S., Schmitz, C., Huber, T., Messerle, B. A., and Otting, G. (2008) A dipicolinic acid tag for rigid lanthanide tagging of proteins and paramagnetic NMR spectroscopy. *J. Am. Chem. Soc. 130*, 10486–10487.

(15) Swarbrick, J. D., Ung, P., Su, X.-C., Maleckis, A., Chhabra, S., Huber, T., Otting, G., and Graham, B. (2011) Engineering of a bis-chelator motif into a protein α-helix for rigid lanthanide binding and paramagnetic NMR spectroscopy. *Chem. Commun. 47*, 7368–7370.

(16) Swarbrick, J. D., Ung, P., Chhabra, S., and Graham, B. (2011) An iminodiacetic acid based lanthanide binding tag for paramagnetic exchange NMR spectroscopy. *Angew. Chem., Int. Ed. 50*, 4403–4406.

(17) Lu, Y., Berry, S. M., and Pfister, T. D. (2001) Engineering novel metalloproteins: design of metal-binding sites into native protein scaffolds. *Chem. Rev. 101*, 3047–3080.

(18) Su, X.-C., Huber, T., Dixon, N. E., and Otting, G. (2006) Site-specific labelling of proteins with a lanthanide-binding tag. *ChemBioChem 7*, 1469–1474.

(19) Su, X.-C., McAndrew, K., Huber, T., and Otting, G. (2008) Lanthanide-binding peptides for NMR measurements of residual dipolar couplings and paramagnetic effects from multiple angles. *J. Am. Chem. Soc. 130*, 1681–1687.

(20) Häussinger, D., Huang, J., and Grzesiek, S. (2009) DOTA-M8: an extremely rigid, high-affinity lanthanide chelating tag for PCS NMR spectroscopy. *J. Am. Chem. Soc. 131*, 14761–14767.

(21) Parker, D., Dickins, R. S., Puschmann, H., Crossland, C., and Howard, J. A. K. (2002) Being excited by lanthanide coordination complexes: aqua species, chirality, excited-state chemistry, and exchange dynamics. *Chem. Rev. 102*, 1977–2010.

(22) Woods, M., Botta, M., Avedano, S., Wang, J., and Sherry, A. D. (2005) towards the rational design of MRI contrast agents: a practical approach to the synthesis of gadolinium complexes that exhibit optimal water exchange. *Dalton Trans. 2005*, 3829–3837.

(23) Dickins, R. S., Parker, D., Bruce, J. I., and Tozer, D. J. (2003) Correlation of optical and NMR spectral information with coordination variation for axially symmetric macrocyclic Eu(III) and Yb(III) complexes: axial donor polarisability determines ligand field and cation donor preference. *Dalton Trans. 2003*, 1264–1271.

(24) Sunnerhagen, M., Nilges, M., Otting, G., and Carey, J. (1997) Solution structure of the DNA-binding domain and model for the binding of multifunctional arginine repressor to DNA. *Nat. Struct. Biol. 4*, 819–826.

(25) Schmitz, C., Stanton-Cook, M. J., Su, X.-C., Otting, G., and Huber, T. (2008) Numbat: an interactive software tool for fitting $\Delta\chi$-tensors to molecular coordinates using pseudocontact shifts. *J. Biomol. NMR 41*, 179–189.

(26) Nguyen, T. H. D., Ozawa, K., Stanton-Cook, M., Barrow, R., Huber, T., and Otting, G. (2011) Pseudocontact shifts in protein NMR spectra generated using a genetically encoded Co^{2+}-binding amino acid. *Angew. Chem., Int. Ed. 50*, 692–694.

(27) Jia, X., Maleckis, A., Huber, T., and Otting, G. (2011) 4,4′-Dithiobis-dipicolinic acid: a small and convenient lanthanide-binding tag for protein NMR spectroscopy. *Chem.—Eur. J. 17*, 6830–6836.

(28) Parker, D., Puschmann, H., Batsanov, A. S., and Senanayake, K. (2003) Structural analysis of nine-coordinate lanthanide complexes: steric control of the metal-water distance across the series. *Inorg. Chem. 42*, 8646–8651.

(29) Cornilescu, G., Marquardt, J. L., Ottiger, M., and Bax, A. (1998) Validation of protein structure from anisotropic carbonyl chemical shifts in a dilute liquid crystalline phase. *J. Am. Chem. Soc. 120*, 6836–6837.

(30) Bertini, I., Janik, M. B. L., Lee, Y. M., Luchinat, C., and Rosato, A. (2001) Magnetic susceptibility tensor anisotropies for a lanthanide ion series in a fixed protein matrix. *J. Am. Chem. Soc. 123*, 4181–4188.

(31) Su, X.-C., and Otting, G. (2010) Paramagnetic labelling of proteins and oligonucleotides for NMR. *J. Biomol. NMR 46*, 101–112.

(32) Su, X.-C., and Otting, G. (2011) Erratum to: Paramagnetic labelling of proteins and oligonucleotides for NMR. *J. Biomol. NMR 50*, 99–100.

(33) Maumela, H., Hancock, R. D., Carlton, L., Reibenspies, J. H., and Wainwright, K. P. (1995) The amide oxygen as a donor group. Metal ion complexing properties of tetra-*N*-acetamide substituted cyclen: a crystallographic, NMR, molecular mechanics, and thermodynamic study. *J. Am. Chem. Soc. 117*, 6698–6707.

(34) Potapov, A., Yagi, H., Huber, T., Jergic, S., Dixon, N. E., Otting, G., and Goldfarb, D. (2010) Nanometer scale distance measurements in proteins using Gd^{3+} spin labeling. *J. Am. Chem. Soc. 132*, 9040–9048.

(35) Aime, S., Barge, A., Batsanov, A. S., Botta, M., Castelli, D. D., Fedeli, F., Mortillaro, A., Parker, D., and Puschmann, H. (2002) Controlling the variation of axial water exchange rates in macrocyclic lanthanide(III) complexes. *Chem. Commun. 2002*, 1120–1121.

(36) John, M., Pintacuda, G., Park, A. Y., Dixon, N. E., and Otting, G. (2006) Structure determination of protein-ligand complexes by transferred paramagnetic shifts. *J. Am. Chem. Soc. 128*, 12910–12916.

(37) Zhuang, T. D., Lee, H. S., Imperiali, B., and Prestegard, J. H. (2008) Structure determination of a Galectin-3-carbohydrate complex using paramagnetism-based NMR constraints. *Protein Sci. 17*, 1220–1231.

(38) Pintacuda, G., Park, A. Y., Keniry, M. A., Dixon, N. E., and Otting, G. (2006) Lanthanide labeling offers fast NMR approach to 3D structure determinations of protein-protein complexes. *J. Am. Chem. Soc. 128*, 3696–3702.